

Hydrogen Atom Transfer in Ribonucleotide Reductase (RNR)

Per E. M. Siegbahn,* Leif Eriksson, Fahmi Himo, and Maria Pavlov

Department of Physics, Stockholm University, Box 6730, S-113 85 Stockholm, Sweden

Received: June 26, 1998; In Final Form: September 25, 1998

The communication between the cysteine, Cys439, at the substrate site and the tyrosyl radical, Tyr122, in ribonucleotide reductase is studied by quantum chemical models at the DFT-B3LYP level. Recent theoretical and experimental studies have indicated that an electron transfer between these sites is highly unlikely. Instead, a model based on the hydrogen atom transfer (HAT) mechanism is investigated. In this mechanism both the proton and electron are moved in each step to avoid a costly charge separation. It is found that the hydrogen atom transfer steps required for communication between Cys439 in R1 and Trp48 in the region of the iron dimer in R2 all have quite low energy barriers. The radical transfer between Tyr731 and Tyr730 has a barrier of 4.9 kcal/mol, while the one between Tyr730 to Cys439 has a barrier of 8.1 kcal/mol. An interesting aspect of these transfers is that the dielectric contribution from the protein is very small, indicating very small charge separations. The radical transfer from Tyr122 to Trp48 over the iron dimer is considerably more complicated. A model is suggested where this transfer occurs in essentially one step by a hydrogen atom transfer from a water ligand of the iron dimer to Tyr122. In this process an electron is transferred between Trp48 to the hydroxyl ligand of iron over the Trp48-Asp237-His241 chain leading to a cationic tryptophan radical.

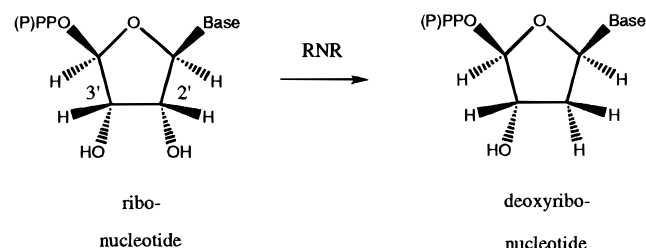
I. Introduction

Ribonucleotide reductase catalyzes the reduction of ribonucleotides to their corresponding deoxyribonucleotides (see Scheme 1).

Although apparently simple, this reaction has been shown to occur in a surprisingly complicated sequence of steps. The present knowledge of RNR has been summarized in recent reviews.^{1,2} There are three classes of RNR. The *Escherichia coli* RNR belongs to Class I and has been shown to be an $\alpha_2\beta_2$ tetramer that can dissociate into two catalytically inactive homodimers, R1 and R2.³ The X-ray structures of both R1^{4,5} and R2⁶ have been determined rather recently.

The mechanism by which RNR catalyzes the reaction in Scheme 1 can be briefly described in the following way. An oxygen molecule is dissociated by an Fe(II,II) dimer complex in R2. For a detailed discussion of the iron dimer complex and its reactions in RNR, see recent reviews.^{7,8} The immediate product of the O₂ dissociation is at present not fully known. One possibility is suggested by the large similarity between the iron dimer complexes in RNR and MMO (methane monooxygenase). For MMO, a complex termed compound **Q** has been identified and shown to react with hydrocarbons. Based on a compilation of experiments,⁹ on DFT calculations¹⁰ and on EXAFS measurements,¹¹ compound **Q** has been suggested to be a bis- μ -oxo Fe(IV,IV) dimer, but there are also other possibilities.¹² For RNR, an intermediate has been observed termed **X**, which is reduced one step compared to **Q**. This intermediate has been spectroscopically characterized as an Fe-(IV,III) dimer.¹³ A possibility is that compound **X** is obtained from compound **Q** through a hydrogen atom (proton and electron) abstraction from surrounding residues. In the next step, a hydrogen atom is abstracted from a tyrosine, Tyr122, fairly close to the iron dimer to create a neutral tyrosyl radical

SCHEME 1



and a resting Fe(III,III) dimer. This is the situation when the ribonucleotide becomes hydrogen bonded at the substrate site in R1. The distance (see Figure 1) between the tyrosyl radical in R2 and the substrate site in R1 is more than 30 Å. These sites are connected by a single hydrogen-bonded chain. The substrate reactions at R1 are initiated by a transfer of radical character from Tyr122 to Cys439 at the substrate site. The transformation shown in Scheme 1 is then catalyzed by the Cys439 radical. Based on isotopic labeling, kinetic, spectroscopic, and site-directed mutagenesis experiments, a reaction mechanism for this part has been suggested¹⁴ consisting of five steps. On the basis of density functional theory (DFT) calculations, another mechanism is suggested consisting of six steps.¹⁵ When the transformation in Scheme 1 is done, the radical is then transferred back to its resting position at Tyr122.

The present study concerns the mechanism for radical transfer between Tyr122 and Cys439. Initially, the mechanism was suggested to be electron transfer followed by local proton transfers to create neutral radicals. In past years, more and more experimental information has been gathered^{1,2} that makes this suggestion rather unlikely. In particular, mutagenesis experiments have been performed that strongly suggest that the hydrogen bonds in the chain shown in Figure 1 are in some way essential for the communication between Tyr122 and Cys439.¹⁶ By means of theoretical DFT studies on simple

* Author to whom correspondence should be addressed.

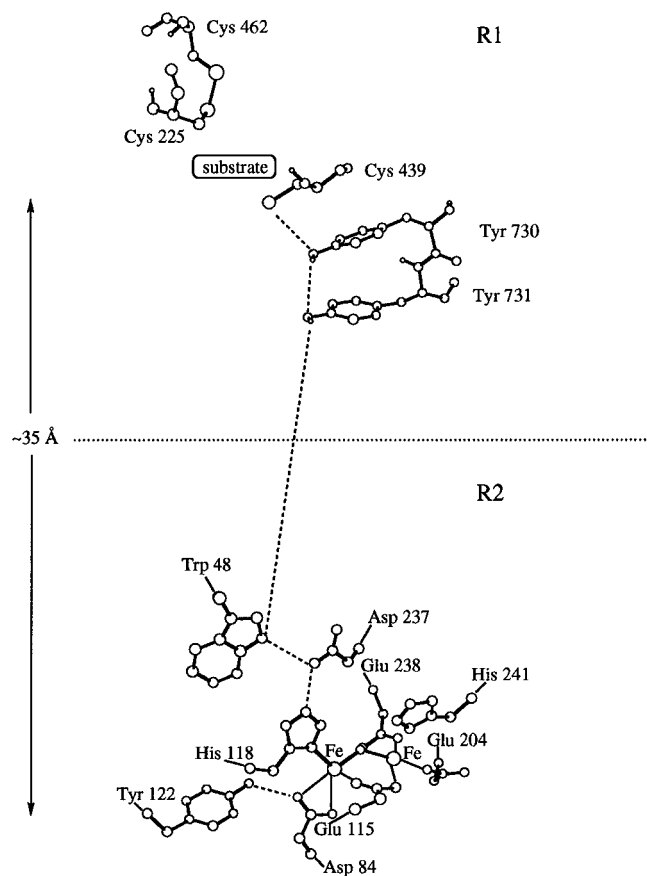


Figure 1. Conserved residues participating in the proposed hydrogen-bonded long-range transfer chain between the substrate site in protein R1 and the tyrosyl radical in protein R2 of *E. coli* ribonucleotide reductase (RNR). The dashed lines indicate possible hydrogen bonds in the crystal structures of the proteins.

amino acid models, an alternative possibility was suggested.¹⁷ In this mechanism entire hydrogen atoms, protons and electrons, are transferred in each step. Three different types of mechanisms were found in the model study. The first one was termed proton-governed hydrogen transfer since the transfer is initiated by a proton transfer, which is then followed by an electron transfer and a final proton transfer. The second possibility was termed overlap-governed hydrogen transfer, since an overlap is needed between the electron donating and electron receiving orbitals. In this case the proton and electron take slightly different paths in each step. Finally, in the third mechanism, the coupling of the electron and proton motion is so strong that a hydrogen atom can be identified during the entire transfer. Common for all three mechanisms is that charge separation is always kept very small and that at each step a hydrogen atom is transferred. The common name for this mechanism is therefore hydrogen atom transfer (HAT). Recently, another DFT study was made which shows that the structure around Cys439 and Tyr122 in RNR is very nonoptimal for electron transfer between these residues.¹⁸ In fact, the results of the calculations are that this electron transfer is so strongly endothermic (by more than 40 kcal/mol) that it is not energetically feasible. In the present study, the hydrogen atom transfer model is investigated in detail for the radical transfer in RNR. The hydrogen-bonded chain in Figure 1 consists of two quite different sections. There is first the region from Cys439 at the substrate site in R1 to the Trp48 residue which is in the neighborhood, although not a direct ligand, to the iron dimer in R2. It is suggested here that the radical transfer in this part of the chain occurs through a sequence of individual steps of

hydrogen atom transfers between amino acid residues. This model will be tested for two cases, first the hydrogen atom transfer between Tyr730 and Tyr731, and second between Cys439 and Tyr730. The mechanism for radical transfer in the second part of the hydrogen-bonded chain, between Tyr122 and Trp48, involving the iron dimer is considerably more complicated and therefore more uncertain. A detailed picture from the X-ray structure⁶ of this region is shown in Figure 2. A model for how the radical transfer in this region could occur is nevertheless suggested below. This mechanism involves, besides a hydrogen atom transfer of the type mentioned above, also a transfer of radical character involving the His118-Asp237-Trp48 chain of the same type as has been experimentally¹⁹ and theoretically²⁰ shown to occur in cytochrome *c* peroxidase (CCP) through the same triad of residues, but involving a heme group rather than an iron dimer as in RNR.

In the present study the hybrid DFT (density functional theory) method B3LYP is used.^{21,22} For benchmark tests comprising 55 common first and second row molecules performed using slightly larger basis sets than used here, an average absolute deviation compared to experiments of 2.2 kcal/mol was obtained for the atomization energies, of 0.013 Å for the bond distances and of 0.62° for the bond angles.²³ The present accuracy should be almost as high as in this benchmark test for the systems that do not contain transition metals. For the latter systems the accuracy should be somewhat lower,²⁴ but should still be enough for the present purposes. For processes such as the ones studied here where charge separations could occur, it is also important to account for long-range polarization effects, and this has been done here using dielectric cavity methods.

II. Computational Details

The calculations were performed in three steps. Following an optimization of the geometry using medium-size basis sets, the energy is evaluated using large basis sets. In the third step the effect of the polarized surrounding was evaluated. All these steps were made at the B3LYP level^{21,22} using the Gaussian-94 program.²⁵

The B3LYP functional can be written as

$$F^{\text{B3LYP}} = (1 - A) * F_x^{\text{Slater}} + A * F_x^{\text{HF}} + B * F_x^{\text{Becke}} + C * F_c^{\text{LYP}} + (1 - C)F_c^{\text{VWN}}$$

where F_x^{Slater} is the Slater exchange, F_x^{HF} is the Hartree-Fock exchange, F_x^{Becke} is the gradient part of the exchange functional of Becke,²¹ F_c^{LYP} is the correlation functional of Lee et al.,²⁶ and F_c^{VWN} is the correlation functional of Vosko et al.²⁷ A , B , and C are the coefficients determined by Becke²¹ using a fit to experimental heats of formation, but Becke did not use F_c^{VWN} and F_c^{LYP} in the expression above when the coefficients were determined, but used the correlation functionals of Perdew and Wang instead.²⁸

In the B3LYP geometry optimizations standard double- ζ basis sets were used. For the metal-containing systems the LANL2DZ set (from Gaussian-94) was used. This basis set uses an ECP (effective core potential)²⁹ for the metal atoms. For the systems composed of only first and second row atoms, the d95 basis set was used. These rather small basis sets can safely be used for the present purposes since it has been clearly shown that the final energy is very insensitive to the quality of the geometry optimization.^{23,30} The B3LYP final energy calculations were made using much larger basis sets. For the metal-containing systems, the LANL2DZ basis set was extended by adding

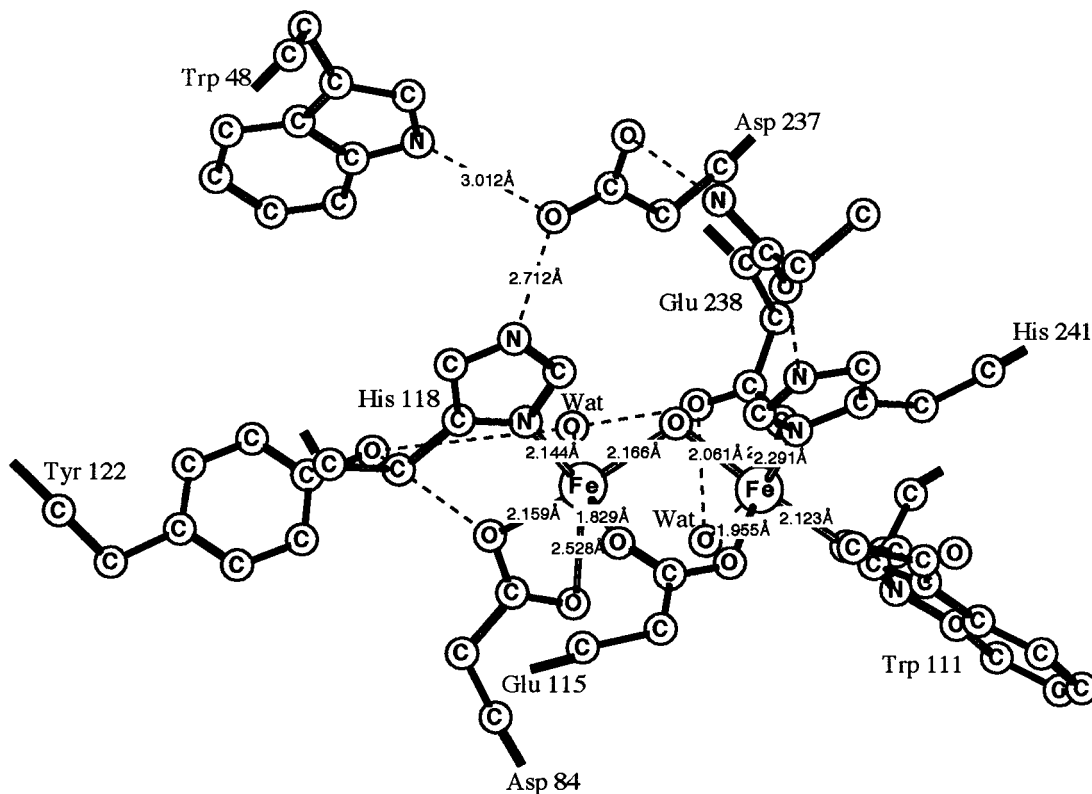


Figure 2. The region around the Fe(III,III) dimer from the X-ray structure of the R2 protein of RNR.

diffuse functions and a single set of polarization functions for all atoms taken from the 6-311+G(1d,1p) basis set. For the systems that do not contain metal atoms, the somewhat larger 6-311G(2df,p) basis set could be afforded. The difference in quality between these large basis sets should be very small for the present type of B3LYP calculations.

The dielectric effects from the surrounding protein were obtained using the self-consistent isodensity polarized continuum model (SCI-PCM) as implemented in the Gaussian-94 program.^{25,31} This is a simple model for treating long-range solvent effects and considers the solvent as a macroscopic continuum with a dielectric constant ϵ and the solute as filling a cavity in this continuous medium. The cavity is defined self-consistently in terms of a surface of constant charge density for the solute molecule. The default isodensity value of $0.0004e/B^3$ was used, which has been found to yield volumes close to the observed molar volumes. The solvent effect is derived from the interactions of the surface potential with the dielectric continuum. The dielectric constant (ϵ) of the protein is the main empirical parameter of the model and it was chosen to be equal to 4, in line with previous suggestions for proteins. This value corresponds to a dielectric constant of about 3 for the protein itself and of 80 for the water medium surrounding the protein. It should be emphasized that with such a simple model of the protein as a dielectric medium, it is absolutely necessary to include important hydrogen-bonding effects in the quantum chemical model.^{18,32} In the present case, the choice of $\epsilon = 4$ can also be motivated by the fact that this value gives good agreement with experiment for two different electron-transfer processes in the bacterial photosynthetic reaction center.³² RNR is similar to this system in terms of water contents and should therefore have a similar dielectric constant.

For the systems not containing metals, zero-point vibrational effects were obtained at the same B3LYP level as the geometries were optimized except in one case. For the hydrogen atom transfer between two tyrosines including the backbone, a Hessian

at this level was found to be too expensive and instead evaluated at the Hartree-Fock level and with the frequencies scaled by 0.9 as usual. For the metal containing systems, differential zero-point vibrational effects are assumed to be small when forms of the same complex are compared. When O-H bond strengths are calculated a zero-point effect of 6.2 kcal/mol was subtracted based on the effect obtained at the B3LYP level for a water ligand in a five coordinated Mn(IV) complex.³³ A systematic basis set and method correction to the O-H bond strength of +1.7 kcal/mol was also added to the values discussed below based on the error obtained for a free water molecule.

III. Results and Discussion

The present model study on hydrogen atom transfer in RNR is divided into two parts which are quite different from a modeling perspective. In the first part, discussed in the first subsection below, hydrogen atom transfer is suggested to occur in steps between individual amino acid residues. This type of transfer should occur once the radical has been transferred from Tyr122 to Trp48, see Figure 1. In the first step after that, the radical is transferred from Trp48 probably to the nearby Tyr356 by a hydrogen atom transfer in the opposite direction. Since the structure of the protein in this region is not very clear, this step is not discussed below. In the following steps, the radical should be transferred between tyrosines. An example of this will be discussed in detail below for the hydrogen atom transfer between Tyr730 and Tyr731. Since these residues are directly linked by the backbone, the effect of the backbone on the transfer will also be discussed. Apart from this case, the backbone is left out of the model calculations. After the sequence of radical transfers between the tyrosines, there should be a final transfer between Tyr730 and Cys439. This step is also discussed in the first subsection. In the second part of this section, the radical transfer involving the metal center in R2 is discussed. Since this part is substantially more complicated than

the cases mentioned above, only a plausible mechanism for this transfer can be suggested. This part of the transfer chain is also too big to be modeled in its entirety by the present quantum chemical methods, and a more approximate modeling is therefore required. The most drastic aspect of the modeling used here is that only one-half of the iron dimer is kept. The bis- μ -oxo bridges are modeled to give the right oxidation state for the iron atom that is kept in the model and which is directly involved in the radical transfer. This transfer is discussed in the second subsection below.

a. Hydrogen Atom Transfers between Amino Acids. The first hydrogen atom transfer between amino acids discussed in this subsection is the one between Tyr730 and Tyr731, which is in the part of the hydrogen-bonded chain that is in R1, see Figure 1. In the previous quantum chemical model study of hydrogen atom transfer,¹⁷ the case of a transfer between two tyrosines was modeled by two vinyl alcohols. The results of these calculations, which had considerable difficulties in converging to a proper transition state, was a barrier of 9.8 kcal/mol corresponding to a rate of 10^5 s^{-1} . The mechanism of the transfer was one of overlap-governed hydrogen transfer (see Introduction) since the vinyl alcohols lined up in a parallel fashion with overlap between the π -orbitals. Placing a water molecule between the vinyl alcohols in a way such that the hydrogen transfer goes via the water, considerably stabilized the transition state. The barrier obtained was 5.4 kcal/mol corresponding to a rate of 10^9 s^{-1} . This led to a suggestion³⁴ that a water molecule in the immediate neighborhood, actually seen in more refined X-ray structures,⁴ takes part in and helps the transfer. It was also shown in these model studies that if a carboxylate group is present in this type of transfer, which is not the case in RNR, the hydrogen atom transfer barrier is reduced even further to 3.0 kcal/mol.

In the previous study of hydrogen atom transfer, the accuracy of the B3LYP method for this type of process was also discussed. This was done partly because the problem with too low barriers using DFT methods had previously been pointed out.^{35,36} Comparison between B3LYP was made to the PCI-80 method,³⁷ which is expected to give barriers too high compared to experiments by 1–2 kcal/mol. The barrier heights obtained using these methods were for the hydrogen transfer reaction between H_2O and CH_3 12.9 (B3LYP) and 14.7 kcal/mol (PCI-80), between OOH and CH_4 20.9 and 22.7 kcal/mol, and between OH and H_2O 4.2 and 5.0 kcal/mol. The conclusion drawn was that B3LYP does work quite well for these reactions, but that the barriers may be slightly too low. This effect is not of any consequence for the conclusions drawn for the present systems.

In the present study tyrosine is modeled by a phenol group which should be a quite accurate model, better than the vinyl alcohol used previously. In the initial attempts to locate a transition state using the phenol model, the same problem as noted previously for the simpler models was encountered. After some fruitless attempts, it was decided to also include the backbone joining Tyr730 and Tyr731 in the model. This led to a larger and therefore more expensive model, but the convergence to the transition state, shown in Figure 3 was much easier. This transition state has some notable features. First, the structure is quite similar to the one of the resting state from the X-ray structure in Figure 1. It is therefore clear that one role of the protein is to hold the phenol rings in a position suitable for the transfer, see further below. Another striking feature of the structure is that the hydrogen atom moves out of the phenol planes with angles of 50.8° and 59.7° with respect

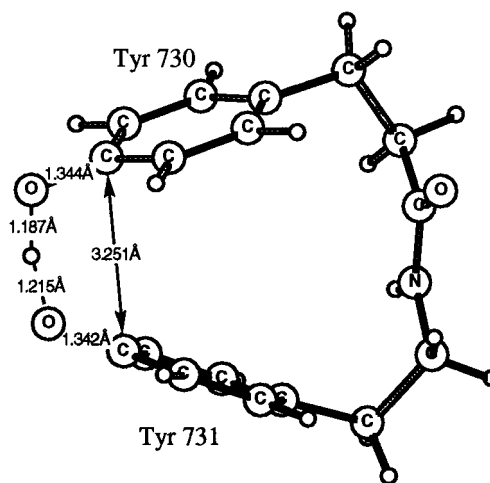


Figure 3. The optimized structure of the transition state for the quantum chemical model for hydrogen atom transfer between Tyr730 and Tyr731.

to the two rings. This is necessary since the tyrosyl radical is a π -radical. By moving out of the σ -plane, the hydrogen orbital can mix with the π -orbitals of the tyrosines and thereby lead to a smooth transfer from one π -radical to the other. The other possibility would have been to move a proton between the tyrosines and let the electron go directly between the π -orbitals. This would require overlap between the π -orbitals and would have corresponded to a mechanism of overlap governed hydrogen transfer as found in the vinyl alcohol case with intermediate groups (water or carboxylate). In that case the shortest distance between the vinyl alcohols was 2.4–2.6 Å, depending on the intermediate group. The shortest distance between the phenol rings in Figure 3 is 3.25 Å, which appears to be too long to give a sufficient direct electron transfer between the rings. Instead, the mechanism in this case is the most clear case of pure hydrogen atom transfer seen so far; a hydrogen atom can be identified along the entire reaction path. The transition state is quite symmetrical, as expected, with O–H distances of 1.19 and 1.22 Å. The C–O distances are both 1.34 Å, which is between the tyrosine value of 1.39 Å and the tyrosyl radical value of 1.31 Å.

The computed barrier for hydrogen atom transfer between Tyr730 and Tyr731 is 4.9 kcal/mol, corresponding to a rate of 10^9 s^{-1} . This rate is substantially faster, as required, than the substrate turnaround time for RNR of 10 s^{-1} . Zero-point vibrational effects and dielectric effects of the protein are included in the barrier height. The zero-point effects are substantial with a lowering of the barrier by 4.6 kcal/mol, from 9.5 kcal/mol to 4.9 kcal/mol. The dielectric effects are quite interesting for this new type of mechanism. If there would be a substantial charge separation as there must be in a pure electron transfer, the dielectric effects should be quite large. If, on the other hand, the electron and proton are close to each other at the transition state, a much smaller effect is expected. The actual result is that dielectric effects only decrease the barrier height by 0.1 kcal/mol. This is one of the most important results of the present study since it clearly demonstrates that this is not simply a variant of electron transfer. This type of result, a very small dielectric effect, is typical for all of the present model systems of hydrogen transfer between amino acids, also for the ones studied previously.¹⁷ An important technical advantage in this context is that the choice of dielectric constant (in the present case $\epsilon = 4$) is not critical at all and that an uncertain and difficult modeling of the protein is not necessary. The hydrogen transfer mechanism shown in Figure 3 is structurally

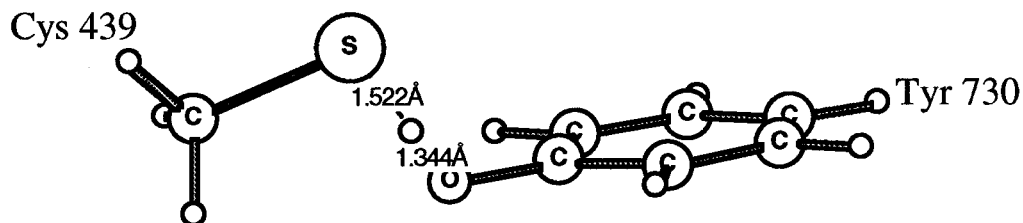


Figure 4. The optimized structure of the transition state for the quantum chemical model for hydrogen atom transfer between Cys439 and Tyr730.

and energetically almost identical in the gas phase and in the protein, and is ideally suited for a treatment using the present accurate DFT methods.

Having obtained the transition state between the tyrosines including the backbone, it should be possible to go back and find the transition state without the backbone. The initial attempts had been unsuccessful, as mentioned above. It turns out that it is still difficult to obtain a stable transition state without the backbone, but finally a reasonably stable structure with small remaining average forces and a Hessian leading to one imaginary frequency was found. The barrier height without the backbone is 9.5 kcal/mol which is much higher than the value of 4.9 kcal/mol obtained with the backbone. The main reason for this is that the structures of the reactants (and products) are quite different without the backbone. The transition state is, on the other hand, very similar.

The second hydrogen transfer described here is the final one in the hydrogen-bonded chain between Cys439 and Tyr730, creating the cysteinyl radical. The transition state obtained is shown in Figure 4, and was much easier to converge than the one between the two tyrosines. It should be noted that the cysteine and the tyrosyl are not oriented quite the same way in the model as they are in the protein, since they are not held in positions by the backbone in the model. This is of no significance for the mechanism or the barrier height, since the rotation around the S–H bond is almost without cost of energy. The calculated barrier is 8.1 kcal/mol, corresponding to a rate of 10^7 s^{-1} , again much faster than the overall reaction rate of RNR. The reaction is found to be only slightly endothermic by 0.4 kcal/mol, which means that the backward hydrogen transfer is almost as fast. The zero-point vibrational effects of -1.7 kcal/mol in the forward direction (toward the cysteinyl radical) are important for the rate, but smaller than for the above reaction between the tyrosines. For the backward reaction they are larger with -4.2 kcal/mol. This is expected, since the large loss of zero-point energy occurs when the O–H bond of tyrosine is entirely broken. The corresponding loss of zero-point energy by breaking the S–H bond is much smaller since the mass of sulfur is larger. The dielectric effects of the protein are quite small, increasing the barrier by 0.3 kcal/mol and increasing the endothermicity by 0.8 kcal/mol. The mechanism of hydrogen transfer thus does not involve any significant charge separation and can be described as hydrogen atom transfer (HAT). This is also supported by the bending angle of 46.4° between the O–H direction and the phenol plane at the transition state, allowing mixing between the π -orbitals and the hydrogen orbital.

Unfortunately, the lack of structural information of part of the hydrogen-bonded chain does not allow any more model calculations of radical transfer between different amino acids to be made. The indication from the structure is that additional hydrogen transfers between tyrosines might occur, possibly involving also Tyr356. The barriers for these should of course be quite similar to the one shown in Figure 3. Instead, the second part of the radical transfer involving the iron dimer complex will be discussed in the next subsection.

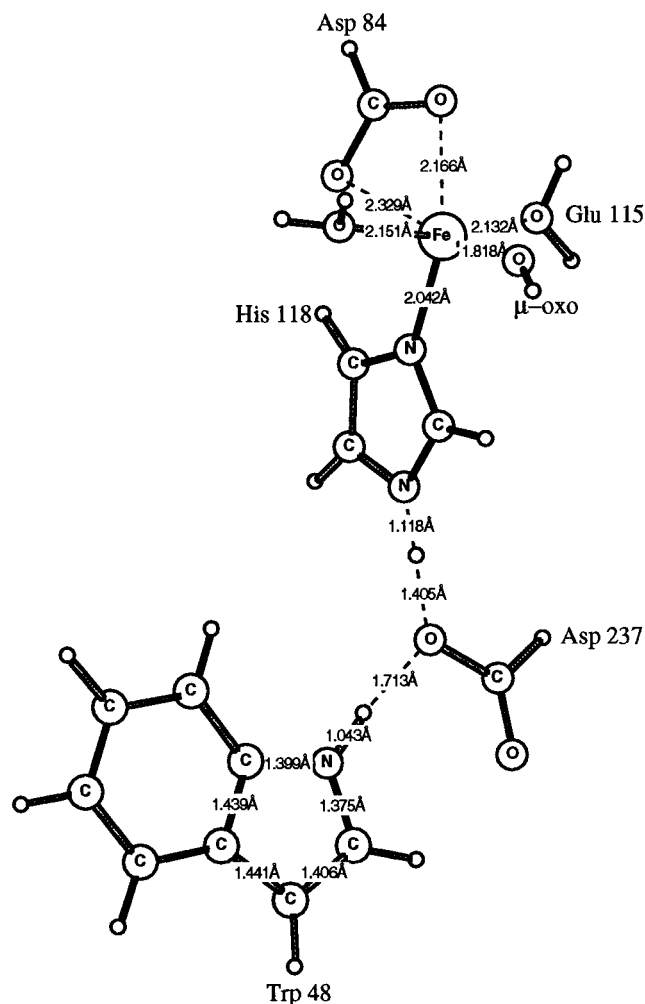


Figure 5. The optimized structure for the quantum chemical model of the iron dimer system in its resting Fe(III,III) state. A water molecule is used to model the Glu115 bridge, and a hydroxyl group models the μ -oxo bridge.

b. Hydrogen Atom Transfer Involving the Iron Complex.

The part of the radical transfer that remains to be discussed is the one between Tyr122 and Trp48 over the iron dimer complex, see Figure 1. The mechanism tested here corresponds to essentially a single step for this entire distance. Since it involves a large number of amino acid residues and also the iron complex, a more approximate modeling is required. After some initial investigations, the model used is the one shown in Figure 5 and Figure 6. As seen there, only half of the iron dimer was kept in the model, and a water molecule is used to model the Glu115 bridge and a hydroxyl group models the μ -oxo bridge. To model radical transfer, it was considered more important to keep the hydrogen-bonded chain including His118, Asp237, and Trp48. One reason this chain is believed to be important in the radical transfer is that in the protein CCP these same amino acids are present and in that case the tryptophan is found to be

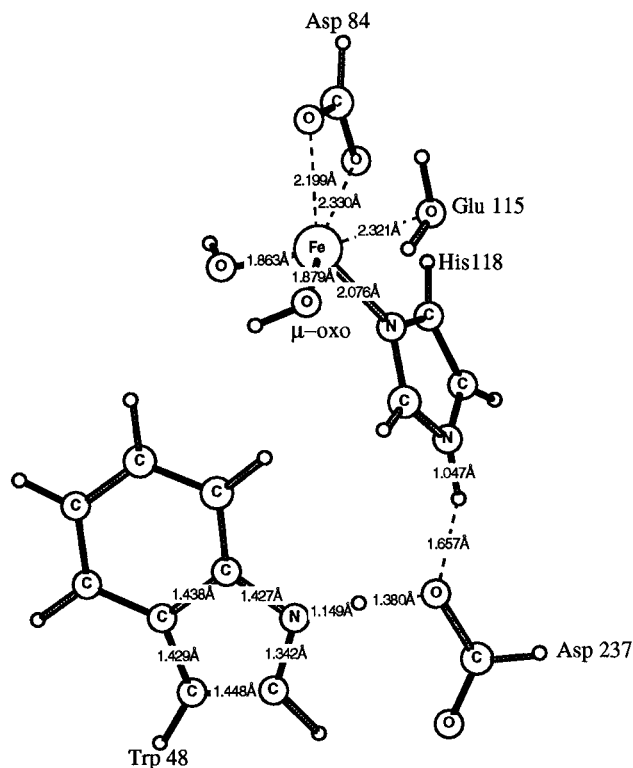


Figure 6. The optimized structure for the quantum chemical model of the iron dimer system at the stage when a hydrogen atom has been abstracted from the iron–water ligand by the Tyr122 radical. A water molecule is used to model the Glu115 bridge, and a hydroxyl group models the μ -oxo bridge.

a radical in the oxidized state.¹⁹ The reactant for the radical transfer investigated is the resting state of the enzyme, which has a Tyr122 radical and an Fe(III,III) dimer complex. In this state a hydrogen bond between the tyrosyl radical and, most probably, the water molecule on the iron atom closest to Tyr122 has been identified for R2 proteins from mouse and HSV1.³⁸ In the product state a hydrogen atom has been abstracted by Tyr122 from this water molecule. Since Tyr122 is not involved further in the radical transfer, it is not included in the model shown in the figures. The energetic effect of the hydrogen abstraction, which is equal to the O–H bond strength of tyrosine, is taken to be the same as the experimental value for phenol of 86.5 ± 2 kcal/mol.³⁹ Since tyrosine is not included in the calculation, no attempt could obviously be made to obtain a transition state like those for the radical transfers in the preceding subsection. This type of optimization was considered too difficult for this process at the present stage.

The optimized model structure for the resting state of the enzyme is shown in Figure 5. A few features of this structure should be pointed out. First, the iron center is six-coordinated with a bidentate binding to the carboxylate, not unlike the bonding in the X-ray structure. The iron oxidation state in the model is Fe(III) as it should be to model the resting Fe(III,III) complex. This is seen on the spin population of 4.00 which is typical for Fe(III) oxidation states.⁴⁰ Also quite typical of highly oxidized iron complexes is the large spin-delocalization over the ligands. The largest spin populations are found on Trp48 with 0.33 and on the hydroxyl group with 0.35. His118 has a spin population of 0.12, but on Asp237 there is no spin.

Concerning the His-Asp-Trp chain, it should first be noted that the fact that only one of the oxygens in the aspartate is involved in hydrogen bonding to the histidine and the tryptophan is adopted directly from the experimental structure (see Figure

2) where the other oxygen is hydrogen bonded to a glutamine. This bonding situation is different from the one in CCP where one oxygen of the aspartate is hydrogen bonded to the histidine and the other to the tryptophan. Since the glutamine of the actual RNR structure is not included in the model, the optimized geometry in Figure 5 is probably only in a local minimum, but this was never tested since the energy difference should anyway be quite small. The optimized N–O distance between His118 and Asp237 is 2.52 Å compared to the experimental value of 2.71 Å, while the N–O distance between Trp48 and Asp237 is 2.75 Å compared to 3.01 Å. The difference in these distances of about 0.3 Å is well reproduced, but the calculated values are somewhat short, which is typical for optimizations using the present basis sets. However, these minor errors should have only very small effects on the calculated energetics. It is further noteworthy that the N–H bond on the histidine is quite long, 1.12 Å, and the O–H distance to the aspartate rather short, 1.41 Å, which are indications of a strong hydrogen bond.

When the tyrosyl radical has abstracted a hydrogen atom from the water coordinated to iron, the product structure shown in Figure 6 is obtained. The coordination around iron in this structure is quite similar to the one in the reactant with six-coordination and a bidentate carboxylate. The spin on iron of 4.04 is also quite similar even though the system has been oxidized, which means that the oxidation state is still Fe(III). This means that a substantial spin population must be present on at least one of the amino acids. Not too surprisingly, from the experimental knowledge of what happens in CCP, most of this spin appears on the tryptophan. For the 7A state, which was the state optimized, the spin on tryptophan is 1.07. There are also large spins of 0.36 and 0.30 on the hydroxyl ligands. Attempts were also made to obtain an Fe(IV) solution, which should correspond to compound X (see Introduction) spectroscopically characterized as an Fe(IV,III) dimer,¹³ but no stable solution was found. Instead, as the geometry convergence progressed, the solution continued down to the more stable Fe(III) solution with a tryptophan radical. However, a metastable Fe(IV) solution was seen in the initial geometry steps with an energy about 10 kcal/mol less stable than the high spin 7A Fe(III) solution. The instability of the Fe(IV) solution seen here, with an energy about 10 kcal/mol higher than that of the Fe(III) solution, is consistent with recent more accurate modeling of compound X using the entire dimer with all of its ligands.⁴¹ In this case an O–H bond strength of 96.4 kcal/mol was obtained for an added hydrogen to compound X, which is about 10 kcal/mol more than the O–H bond strength of tyrosine, indicating an instability of the same magnitude. This means that the radical transfer from Tyr122 to Cys439 in RNR should not go via a compound X solution of the iron dimer but through an unoxidized Fe(III) solution with a tryptophan radical, which is an important result.

From the energies for the structures in Figures 5 and 6, an O–H bond strength of the water coordinated to iron can be obtained. The result is 82.4 kcal/mol, which is quite close to the O–H bond strength of tyrosine of 86.5 kcal/mol. This result means that a hydrogen atom transfer from the coordinated water to the tyrosyl radical is quite feasible energetically, and that in this simple process, the radical is transferred all the way from Tyr122 to Trp48. From the hydrogen-transfer model calculations discussed in the previous subsection, the barrier for this process is furthermore expected to be quite low, but this remains to be shown. If the exact result of the calculations should be taken literally it would also mean that the tyrosine would spontaneously abstract a hydrogen atom from the water, which

is not what happens in the actual RNR system where the tyrosyl radical is in the resting state. However, the present modeling should clearly be regarded as quite approximate considering the size of this system, and a few kcal/mol error must be expected. The most severe modeling approximation is probably that only one-half of the iron dimer is kept.

The calculated O–H bond strength of 82.4 kcal/mol includes an interesting dielectric effect, which increases the bond strength by as much as 9.6 kcal/mol. This effect is the largest one we have so far obtained for any process which preserves electro-neutrality. This means that the protein surrounding, here modeled by a medium with dielectric constant equal to 4, is of significant importance in keeping the O–H bond strength close to the one in tyrosine as is required for the hydrogen atom transfer. The fact that the protein *increases* the O–H bond strength is also quite interesting. The most important changes of the Mulliken charges in this process are that tryptophan goes from +0.20 to +0.73 and that the water ligand (the one that loses a hydrogen to the tyrosine) changes from +0.16 to –0.36. Given the qualitative aspect of the charge concept, these values reasonably indicate that an electron has been transferred from tryptophan to the water ligand as water loses a hydrogen atom to tyrosine. It should be noted that the tyrosine does not accept any charge during this process since in the present model it is neutral before and after the hydrogen transfer. Normally, the protein is expected to make electron transfers such as the one from tryptophan to water easier, but in this case the effect is the opposite. This is due to a very large polarity of the complex before the electron transfer (the dipole moment of the structure in Figure 5 is 11.1 D), which is in fact larger than after the transfer (the dipole moment of the structure in Figure 6 is 7.6 D). It should finally be pointed out in this context that the present chemical model is only qualitative. Besides the simplification of keeping only one iron atom, also some part of the hydrogen bonding, for example to Asp237, has been left out. It is quite possible that a larger, more realistic model where these effects are included should stabilize charge separation even further and thereby change the energetics of the radical transfer somewhat.

In the radical transfer discussed above, the radical has moved from Tyr122 to Trp48 in one single hydrogen atom transfer from a water ligand of the iron dimer to Tyr122. A remaining question is whether the radical character in the region around Trp48 is strong enough to abstract a hydrogen atom from some neighboring amino acid residue. According to what is known about the structure of RNR in this region, this amino acid should probably be Tyr356. To investigate this question a hydrogen atom is added to the structure in Figure 7. This hydrogen atom cannot be added directly to the tryptophan since it is already protonated. Instead it is added to the aspartate, and the structure shown in Figure 7 is obtained. The calculated O–H binding energy of this hydrogen atom is 84.6 kcal/mol, again quite close to the O–H bond strength of tyrosine of 86.5 kcal/mol. Unlike the hydrogen transfer from the water ligand discussed above, there is almost no dielectric effect in this process, only +1.0 kcal/mol on the O–H bond strength. This low effect is not immediately obvious since the charge on tryptophan goes from +0.73 to +0.05 and the one on aspartate from –0.67 to +0.03, clear indications of an electron transfer from the aspartate to the tryptophan. However, the result is in line with our previous experience that local charge transfers over short distances are well handled by the quantum chemical gas-phase models provided they are large enough, like the present ones. The calculated O–H bond strength of 84.6 kcal/mol means that once

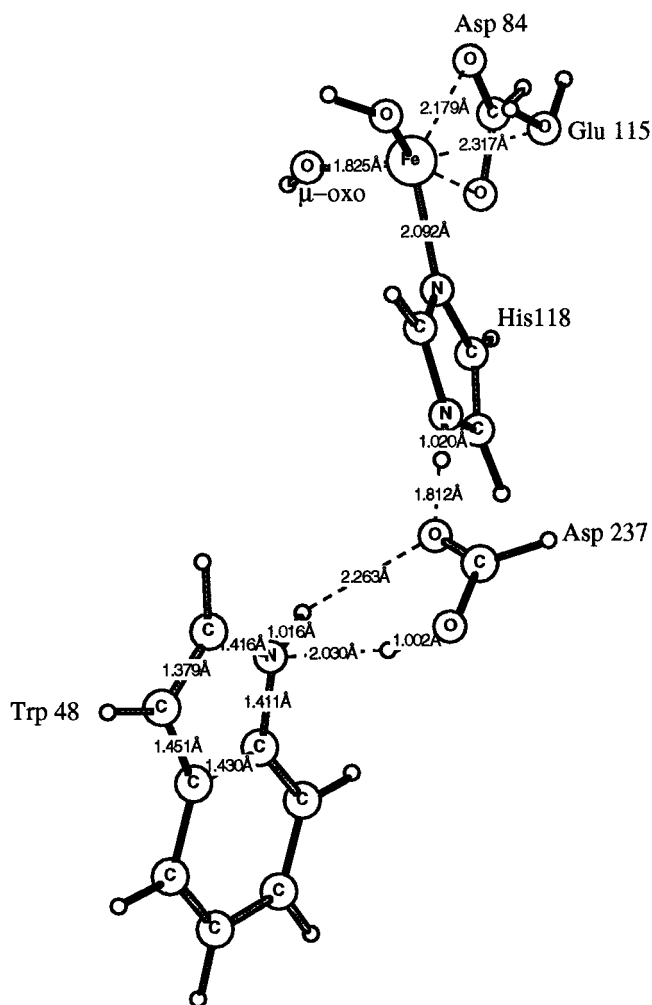


Figure 7. The optimized structure for the quantum chemical model of the iron dimer system at the stage when a hydrogen atom has been abstracted from the iron–water ligand by the Tyr122 radical, and a hydrogen atom has also been abstracted by Asp237 from the nearby Tyr356. A water molecule is used to model the Glu115 bridge, and a hydroxyl group models the μ -oxo bridge.

Tyr122 has abstracted a hydrogen atom from the coordinated water and the radical is transferred to Trp48, the radical can in turn be transferred to Tyr356 by a second hydrogen atom transfer. In the sequence of hydrogen atom transfers discussed in the previous subsection involving Tyr731 and Tyr730, the radical can then finally be transferred to Cys439 at the substrate site.

IV. Conclusions

The present quantum chemical model calculations have shown that a radical transfer between Tyr122 in R2 and Cys439 at the substrate site is energetically quite feasible through a sequence of hydrogen atom transfer steps. The calculated barrier for hydrogen atom transfer between Tyr730 and Tyr731 is only 4.9 kcal/mol while the one between Cys439 and Tyr730 is somewhat higher with 8.1 kcal/mol. These barriers lead to predicted rates of 10^9 s^{-1} and 10^7 s^{-1} , respectively, both much faster than the overall substrate turnaround rate for RNR of 10 s^{-1} . These fast rates give a good rationalization for why the protein only has a single hydrogen-bonded chain between Tyr122 and Cys439 and also why mutations that severely disrupt the hydrogen bonding in this chain stop substrate activity. In particular, mutations substituting Tyr730 and Tyr731 by phenylalanines lead to a total loss of activity, even though π -orbital overlap is retained.¹⁶

An interesting aspect of the calculations is that these hydrogen atom transfers between amino acid residues do not give rise to any polarization effects of the protein. The effects obtained from the dielectric continuum model using $\epsilon = 4$ for the transfer between the tyrosines is only 0.1 kcal/mol and between cysteine and tyrosine only 0.3 kcal/mol. These results indicate that the charge separations occurring in these processes are very small and that these processes therefore are true hydrogen atom transfers.

The radical transfer between Tyr122 and Trp48 over the iron dimer is considerably more complicated. The present model calculations suggest that this transfer occurs in essentially a single step with a hydrogen atom moving from a water ligand of the iron dimer to the Tyr122 radical. In this process there is a large charge transfer from Trp48 to the hydroxyl group at the iron dimer of about 0.5 electrons, leading to a product Trp48 cationic radical. The electron transfer goes over the Trp48-Asp237-His241 chain and is analogous to a similar electron transfer in CCP.¹⁹ Due to the large charge transfer in this step there is a considerable dielectric effect on the O—H bond strength of the water ligand of 9.6 kcal/mol. However, the effect is in the opposite direction from what might have been expected, stabilizing the reactant before the electron transfer more than the product. The iron dimer retains its Fe(III,III) resting state during this step and also during the other steps of the radical transfer. The Fe(IV,III) state is estimated to be about 10 kcal/mol less stable than the diferric state with a Trp48 radical.

In contrast to the present radical transfer mechanism based on transferring entire hydrogen atoms in each step, a pure electron transfer mechanism has recently been shown to be energetically unfeasible.¹⁸ Using a dielectric model previously shown to give very good agreement for electron transfer in the bacterial photosynthetic reaction center, the electron transfer from Cys439 to Tyr122 was shown to be endothermic by more than 40 kcal/mol. The reason for this is mainly that cysteine is a quite poor electron donor, particularly in the surrounding present at the substrate site in RNR.

References and Notes

- (1) Sjöberg, B. M. *Structure* **1994**, *2*, 793–796. Sjöberg, B.-M. *Structure and Bonding* **1997**, *88*, 139–173.
- (2) Gräslund, A.; Sahlin, M. *Annu. Rev. Biophys. Biomol. Struct.* **1996**, *25*, 259–286.
- (3) Reichard, P. *Science* **1993**, *260*, 1773–1777.
- (4) Uhlin, U.; Eklund, H. *Nature* **1994**, *370*, 533–539.
- (5) Eriksson, M.; Uhlin, U.; Ramaswamy, S.; Ekberg, M.; Regnström, K.; Sjöberg, B.-M.; Eklund, H. *Structure* **1997**, *5*, 1077–1092.
- (6) Nordlund, P.; Sjöberg, B.-M.; Eklund, H. *Nature* **1990**, *345*, 593–598.
- (7) Feig, A. L.; Lippard, S. J. Reactions of non-heme. *Chem. Rev.* **1994**, *94*, 759.
- (8) Wallar, B. J.; Lipscomb, J. D. *Chem. Rev.* **1996**, *96*, 2625.
- (9) Shteinman, A. A. *FEBS Lett.* **1995**, *362*, 5–9.
- (10) Siegbahn, P. E. M.; Crabtree, R. H. *J. Am. Chem. Soc.* **1997**, *119*, 3103.
- (11) Shu, L.; Nesheim, J. C.; Kauffmann, K.; Munck, E.; Lipscomb, J. D.; and Que, L., Jr. *Science* **1997**, *275*, 515.
- (12) Riggs-Gelasco, P. J.; Shu, L.; Chen, S.; Burdi, D.; Huynh, B. H.; Que, L., Jr.; Stubbe, J. *J. Am. Chem. Soc.* **1998**, *120*, 849–860.
- (13) Sturgeon, B. E.; Burdi, D.; Chen, S.; Huynh, B.-H.; Edmondson, D. E.; Stubbe, J.; Hoffman, B. M. *J. Am. Chem. Soc.* **1996**, *118*, 7551–7557.
- (14) Stubbe, J. *Biol. Chem.* **1990**, *265*, 5330. Mao, S. S.; Holler, T. P.; Yu, G. X.; Bollinger, J. M.; Booker, S.; Johnston, M. I.; Stubbe, J. *Biochemistry* **1992**, *31*, 9733–9743.
- (15) Siegbahn, P. E. M. *J. Am. Chem. Soc.* **1998**, *120*, 8417.
- (16) Ekberg, M.; Sahlin, M.; Eriksson, M.; Sjöberg, B. M. *J. Biol. Chem.* **1996**, *271*, 20655; Ekberg, M.; Pötsch, S.; Sandin, E.; Thunnissen, M.; Nordlund, P.; Sahlin, M.; Sjöberg, B. M. Manuscript submitted to *J. Biol. Chem.*
- (17) Siegbahn, P. E. M.; Blomberg, M. R. A.; Crabtree, R. H. *Theor. Chem. Acc.* **1997**, *97*, 289–300.
- (18) Siegbahn, P. E. M.; Blomberg, M. R. A.; Pavlov, M. *Chem. Phys. Lett.* **1998**, *292*, 421–430.
- (19) Sivaraja, M.; Goodwin, D. B.; Smith, M.; Hoffman, B. M. *Science* **1989**, *245*, 738.
- (20) Pavlov, M.; Siegbahn, P. E. M.; Blomberg, M. R. A. To be submitted.
- (21) Becke, A. D. *Phys. Rev.* **1988**, *A38*, 3098. Becke, A. D. *J. Chem. Phys.* **1993**, *98*, 1372. Becke, A. D. *J. Chem. Phys.* **1993**, *98*, 5648.
- (22) Stevens, P. J.; Devlin, F. J.; Chablowski, C. F.; Frisch, M. J. *J. Phys. Chem.* **1994**, *98*, 11623.
- (23) Bauschlicher, C. W., Jr; Ricca, A.; Partridge, H.; Langhoff, S. R. In *Recent Advances in Density Functional Methods, Part II*; Chong, D. P., Ed.; World Scientific Publishing Company: Singapore, 1997; p 165.
- (24) Blomberg, M. R. A.; Siegbahn, P. E. M.; Svensson, M. *J. Chem. Phys.* **1996**, *104*, 9546.
- (25) Frisch, M. J.; Trucks, G. W.; Schlegel, H. B.; Gill, P. M. W.; Johnson, B. G.; Robb, M. A.; Cheeseman, J. R.; Keith, T.; Petersson, G. A.; Montgomery, J. A.; Raghavachari, K.; Al-Laham, M. A.; Zakrzewski, V. G.; Ortiz, J. V.; Foresman, J. B.; Cioslowski, J.; Stefanov, B. B.; Nanayakkara, A.; Challacombe, M.; Peng, C. Y.; Ayala, P. Y.; Chen, W.; Wong, M. W.; Andres, J. L.; Replogle, E. S.; Gomperts, R.; Martin, R. L.; Fox, D. J.; Binkley, J. S.; Defrees, D. J.; Baker, J.; Stewart, J. P.; Head-Gordon, M.; Gonzalez, C.; Pople, J. A.; *Gaussian-94 Revision B.2*; Gaussian Inc.: Pittsburgh, PA, 1995.
- (26) Lee, C.; Yang, W.; Parr, R. G. *Phys. Rev.* **1988**, *B37*, 785.
- (27) Vosko, S. H.; Wilk, L.; Nusair, M. *Can. J. Phys.* **1980**, *58*, 1200.
- (28) Perdew, J. P.; Wang, Y. *Phys. Rev. B* **1992**, *45*, 13244. Perdew, J. P. In *Electronic Structure of Solids*; Ziesche, P., Eischrig, H., Eds.; Akademie Verlag: Berlin, **1991**. Perdew, J. P.; Chevary, J. A.; Vosko, S. H.; Jackson, K. A.; Pederson, M. R.; Singh, D. J.; Fiolhais, C. *Phys. Rev. B* **1992**, *46*, 6671.
- (29) Hay, P. J.; Wadt, W. R. *J. Chem. Phys.* **1985**, *82*, 299.
- (30) Siegbahn, P. E. M. *Adv. Chem. Phys.* Vol. XCIII; Prigogine, I., Rice, S. A., Eds.; J. Wiley: New York, 1996; p 333.
- (31) Wiberg, K. B.; Rablen, P. R.; Rush, D. J.; Keith, T. A. *J. Am. Chem. Soc.* **1995**, *117*, 4261. Wiberg, K. B.; Keith, T. A.; Frisch, M. J.; Murcko, M. *J. Phys. Chem.* **1995**, *99*, 9072.
- (32) Blomberg, M. R. A.; Siegbahn, P. E. M.; Babcock, G. T. *J. Am. Chem. Soc.* **1998**, *120*, 8812–8824.
- (33) Blomberg, M. R. A.; Siegbahn, P. E. M. *Mol. Phys.*, in press.
- (34) Siegbahn, P. E. M. In *Molecular Modeling and Dynamics of Bioinorganic Systems*; Comba, P., Banci, L., Eds.; Kluwer Academic Publishers: Norwell, MA, 1997; p 233–253.
- (35) Baker, J.; Andzelm, J.; Muir, M.; Taylor, P. R. *Chem. Phys. Lett.* **1995**, *237*, 53–60.
- (36) Baker, J.; Muir, M.; Andzelm, J. *J. Chem. Phys.* **1995**, *102*, 2063–2079.
- (37) Siegbahn, P. E. M.; Blomberg, M. R. A.; Svensson, M. *Chem. Phys. Lett.* **1994**, *223*, 35. Siegbahn, P. E. M.; Svensson, M.; Boussard, P. J. E. *J. Chem. Phys.* **1995**, *102*, 5377.
- (38) van Dam, P. J.; Willems, J.-P.; Schmidt, P. P.; Pötsch, S.; Barra, A.-L.; Hagen, W. R.; Hoffman, B. M.; Andersson, K. K.; Gräslund, A. *J. Am. Chem. Soc.*, in press.
- (39) Kerr, J. A. In *Handbook of Chemistry and Physics*, 77th ed.; Chemical Rubber Company: Cleveland, 1996; pp 9–51.
- (40) Blomberg, M. R. A.; Siegbahn, P. E. M. *Theor. Chem. Acc.* **1997**, *97*, 72–80.
- (41) Siegbahn, P. E. M. To be submitted.